Ultra low dark count InGaAs/InP single photon avalanche diode

Bin Li †, Yuxiu Niu, Yinde Feng, Xiaomei Chen

Accelink Technologies Co., LTD, Wuhan 430000, China

Abstract: A low noise InGaAs/InP single photon avalanche diode is demonstrated. The device is based on planar type separate absorption, grading, charge and multiplication structure. Relying on reasonably designed device structure and low-damage Zn diffusion technology, excellent low-noise performance is achieved. Due to its importance, the physical mechanism of dark count is analyzed through performance characterization at different temperatures. The device can achieve 20% single photon detection efficiency and 3.2E-7/ns dark count rate with a low after pulsing probability of 0.57% at 233K. This is, to the best of our knowledge, the lowest DCR reported at the same condition.

Keywords: InGaAs/InP; Single photon avalanche diode; dark count;

PACS : 85. 60. Gz, 73. 40. Kp, 81. 15. Hi

EEACC: 7230C

1. Introduction

InGaAs/InP single-photon avalanche photodiode (SPAD) has the advantages of good performance, low cost, small size, and no need for ultra-low temperature cooling. It is the mainstream technical solution and mainstream technology development direction for single-photon detection in the near-infrared band [1]. It is widely applied to the fields of quantum communication and quantum information [2], laser detection and laser imaging [3,4], molecular luminescence and quantum spectroscopy analysis [5]. Especially with the rapid development of quantum secure communication, InGaAs/InP SPAD has become a research and development hotspot [6]. The planar InP-based separate absorption, grading, charge and multiplication (SAGCM) structure is widely adopted in this application due to its high reliability, low noise, high quantum efficiency over a wide spectral region and high gain-bandwidth product [7]. In recent years, with the development of material quality and chip structure, the performance of InGaAs/InP SPAD has been greatly improved. It can reach 20% photon detection efficiency (PDE) at a wavelength of 1.55μm and 1kHz level dark count rate (DCR) at -40～-50℃ [8,9]. However, the application requirements for its performance are still improving. Thus, the development of higher performance devices is of great significance.

Two main types of noise exist in SPAD, dark count (DC) and after pulsing (AP). DCR is the total DC in 1 second, and after pulsing probability (APP) is the ratio of

† Correspondence to: **Bin Li,** E-mail: lbatcq@163.com

after pulsing count to photon count. DC is the intrinsic noise of SPAD, which limits device performance in all application scenarios. While AP becomes important only in high frequency application scenarios. Thus, understanding the physical mechanism and analyzing the source of DC is important for the development of high-performance devices.

2. Experiment

In this letter, a bottom illuminated SAGCM planar structure InGaAs/InP SPAD with very low noise is demonstrated. The epitaxial structure of the InGaAs/InP SPAD is designed as shown in Fig.1. It is grown by metal-organic chemical vapor phase deposition (MOCVD) on n-InP substrate. The structure consists of a InP buffer layer, an undoped InGaAs absorption layer, three undoped InGaAsP grading layers which are used to prevent hole pile up at the heterointerface between InGaAs and InP, a Si doped InP charge layer, and an undoped InP cap layer.

To prevent edge breakdown, low-damage Zn diffusion technology is used to form a stepped structure, which can gradually weaken the edge electric field strength. Zn diffusion depth can be expressed as

$$d = A * \mathrm{sqrt}(t) \tag{1}$$

Where d is the Zn diffusion depth, t is the diffusion time and A is a function of the diffusion condition and material. By fixing the diffusion condition and changing the diffusion time, different Zn diffusion depth can be obtained. By controlling the diffusion process, Zn diffuses deeper in the center region than in the peripheral region, and the thickness of the multiplication layer is controlled to be about 1μm. In this condition, by solving Poisson's equation, it can be found that the electric field under the center region is higher than the periphery region, indicating that edge breakdown is suppressed.

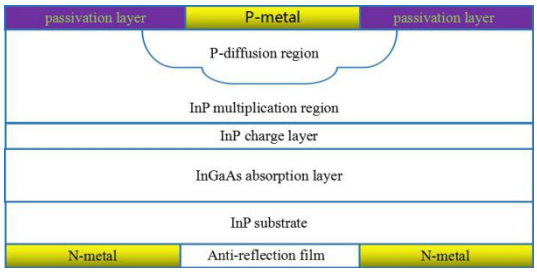

Fig. 1. Schematic diagram of planar type InGaAs/InP SPAD.

3. Results and discussion

The chips are packaged into a coaxial structure with a pigtail to receive the single photon optical signal. Then, the performance is measured at different temperatures and different voltages. The test gate frequency is 1 MHz with a gate voltage of 6V and gate width of 4.4ns, the optical pulse frequency is 100kHz with 1 average photon per optical pulse, and the optical wavelength is 1.55μm.

Fig.2 and Fig.3 shows the typical DCR and after pulsing probability (APP) characteristics as a function of PDE of a device at 233K. DCR is caused by dark

carriers without photon signal, which is the basic noise of the device. Thus, analyzing its generation mechanism is beneficial to research high performance chips . APP is caused by trapping and releasing carriers generated by avalanche process in the multiplication, and it is important in high frequency application scenarios. In this article, APP is calculated the sum of false counts caused by carrier trap and release of the 9 gates after the optical pulse. The highest PDE is 32.6%, which is limited by the low gate voltage. The DCR and APP increase faster than PDE, which means that the device performance cannot be improved by indefinitely increasing the bias voltage.

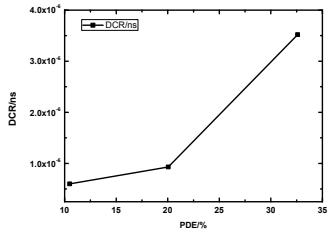

Fig. 2. Dark count rate as a function of photon detection efficiency.

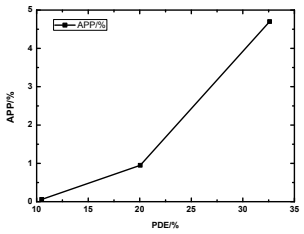

Fig. 3. After pulsing probability as a function of photon detection efficiency.

Fig.4 shows the typical DCR-Temperature characteristics of a device at a PDE of 20%. The DCR increases exponentially with temperature for about one order of magnitude every 30 degrees.

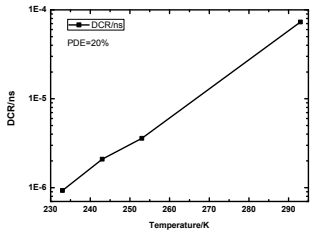

Fig. 4. Dark count rate as a function of operating temperature.

DCR can be caused by dark carriers generated through tunneling in the multiplication region or SRH in the absorption region.

Dark carriers generated through SRH in the absorption region is expressed as

$$N_{SRH} = \frac{n_i}{\tau_{\mathrm{SRH}}} \tag{2}$$

Where τ_{SRH} is the carrier lifetime, and n_i is the intrinsic carrier concentration which is expressed as

$$n_i = \sqrt{N_C * N_V} * \exp(-\frac{E_g}{2*k*T}) \tag{3}$$

Where E_g is the material band gap energy, N_c and N_v are the effective density of states of the conduction band and the valence band, k is the Boltzmann's constant and T is the temperature of the lattice. N_c and N_v are Proportional to $T^{\wedge 1.5}$, the scale factor is sat to be 38.5/(μm^3*K^1.5) for N_c and 1600/(μm^3*K^1.5) for N_v while the accuracy of the scale factor does not affect the conclusion. For InGaAs, E_g is a function of temperature [10]:

$$E_g = 0.819 - (\frac{2.73\mathrm{E}-4}{T+300} + \frac{2.22\mathrm{E}-4}{T+271}) * T^2 \tag{4}$$

The calculated n_i as a function of temperature is plotted in Fig.5. As can be seen, n_i increases about one order of magnitude every 30 degrees, which agree well with DCR-T characteristic of the device. In fact, when the carrier lifetime is set to 90us～1600 us, the simulation DCR result is in good agreement with the test DCR result.

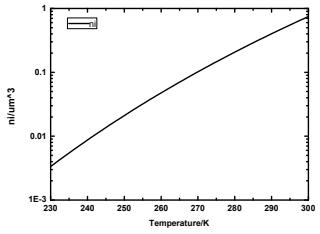

Fig. 5. n_i-T characteristic of the absorption layer.

The dark carrier generation rate per unit volume through band-to-band tunneling is expressed as Equation 5, and through trap assisted tunneling is expressed as Equation 6:

$$N_{\mathrm{bbt}} = \frac{\sqrt{2m_r}q^2E^2}{4\pi^3\hbar^2\sqrt{E_g}} \exp(-\frac{\pi\sqrt{m_r}E_g^{3/2}}{2\sqrt{2}qE\hbar}) \tag{5}$$

$$N_{TAT} = \frac{\sqrt{\frac{2m_r}{E_g}}\frac{q^2\mathrm{E}^2}{4\pi^3\hbar^2}N_{Trap}\exp(-\frac{\pi\sqrt{m_{lh}E_{B1}^3}+\pi\sqrt{m_eE_{B2}^3}}{2\sqrt{2}q\hbar\mathrm{E}})}{N_v\exp(-\frac{\pi\sqrt{m_{lh}E_{B1}^3}}{2\sqrt{2}q\hbar\mathrm{E}})+N_c\exp(-\frac{\pi\sqrt{m_eE_{B2}^3}}{2\sqrt{2}q\hbar\mathrm{E}})} \tag{6}$$

Where $\boldsymbol{E}$ is the electric field strength, m_e=0.08m_0 is the effective electron mass, m_0 is the free-electron mass, m_{lh}=0.089m_0 is the effective light-hole mass, N_{Trap} is the trap concentration, E_{B1} and E_{B2} are the barrier heights from the valence band to the trap and from the trap to the conduction band, respectively. According to the research results of McIntosh [11], for InP, E_{B1}=0.75E_g, E_{B2}=0.25 E_g. Carrier reduced effective mass m_r is expressed as：

$$m_{\mathrm{r}} = \frac{2m_e * m_{lh}}{m_e + m_{lh}} \tag{7}$$

For a multiplication region width of about 1μm, dark carriers generated through

tunneling increase about 20 times while the temperature increases from 220K to 300K [12], which is much slower than DCR.

Thus, DCR is meanly caused by dark carriers generated through SRH in the absorption region.

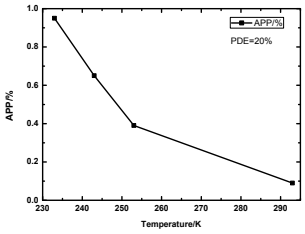

Fig. 6. After pulsing probability versus temperature.

Fig.6 shows the typical APP-Temperature characteristics of a device. The APP decreases with temperature, which means that the lifetime of the trapped carriers decreases with temperature.

Fig.7 shows the DCR and APP characters of 17 devices at 233K. The PDE is 20%. As can be seen, the lowest DCR is 3.2E-7/ns (about 1 count per second in our test system) with APP of 0.57% at the same time, while the lowest APP is 0.38% with DCR of 3.6E-7/ns at the same time. Such a low noise is an evidence of high-quality crystal growth, good edge breakdown suppression and low damage processing. At the same time, both DCR and APP diverse more than one order of magnitude as shown in fig.6. Which may indicate that device performance is strongly dependent on crystal quality and process damage.

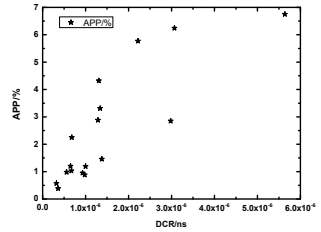

Fig. 7. After pulsing probability and dark count rate of 17 devices.

4. Conclusion

In summary, we have demonstrated a planar structure InGaAs/InP single photon avalanche photodiode which is fabricated by Zn diffusion. At 233K and 20% photon detection efficiency, the dark count rate can be as low as 3.2E-7/ns, and the after pulsing probability can be as low as 0.57% at the same time.

References

[1] J Zhang, M A Itzler, S Zbinden, et al. Advances in InGaAs/InP single photon detector systems for quantum communication. Light: Science & Applications, 2015, 4:e286.

[2] Z Q Ma , Z Wu, Y Xu. Compact SPAD pixels with fast and accurate photon

counting in the analog domain. Journal of Semiconductors, 2021, 42:052402.
[3] C Yu, M Shangguan, H Xia, et al. Fully integrated free-running InGaAs/InP single-photon detector for accurate lidar applications. Optics Express, 2017, 25:14611.
[4] Y R Wang, L L Wang, C Y Wu, et al. Ultra-low detection delay drift caused by the temperature variation in a Si-avalanche-photodiode-based single-photon detector. Chinese Optics Letters, 2021, 19:082502.
[5] M H Lee, C Ha, H S Jeong. Wavelength-division-multiplexed InGaAs-InP avalanched photodiodes for quantum key distribution. Opt. Commun. 2016, 361:162-167.
[6] G J Fan-Yuan, J Teng, S Wang, et al. Optimizing Single-Photon Avalanche Photodiodes for Dynamic Quantum Key Distribution Networks. Physical Review Applied, 2020, 13:054027.
[7] M Sanzaro, S Calandri, A Ruggeri. InGaAs-InP SPAD with monolithically integrated Zinc-diffused resistor. IEEE JOURNAL OF QUANTUM ELECTRONICS, 2016, 52(7):4500207.
[8] X Jiang, M Itzler, K Donnell. InP-based single-photon detectors and Geiger-mode APD arrays for quantum communications applications. IEEE JOURNAL OF SELECTED TOPICS IN QUANTUM ELECTRONICS, 2015, 21(3):3800112.
[9] F Signorelli, F Telesca, E Conca, et al. Low-Noise InGaAs/InP Single-Photon Avalanche Diodes for Fiber-Based and Free-Space Applications. IEEE JOURNAL OF SELECTED TOPICS IN QUANTUM ELECTRONICS, 2022, 28:38013101.
[10] S Paul, J B Roy, and P K Basu. Empirical expressions for the alloy composition and temperature dependence of the band gap and intrinsic carrier density in GaxIn1-xAs. Journal of Applied Physics 1991, 69, 827
[11] K A McIntosh, J P Donnelly, D C Oakley. InGaAs/InP avalanche diodes for photon counting at 1.06μm. Applied Physics Letters, 2002, **81**(14):2505.
[12] B Li, W Chen, X F Huang, et al.. InP cap layer doping density in InGaAs/InP single-photon avalanche diode. J. Infrared Millim. Waves 2017, **36:** 042

Bin Li got his BS from Shandong University in 2009, and Ph.D degree in 2014 at Institute of Semiconductors, Chinese Academy of Sciences. Now he is a senior engineer of Accelink Technologies Co., LTD, graduate Supervisor of Wuhan Academy of Posts and Telecommunications. Research area focuses on InP-based Semiconductor devices.